High-pressure phases of VO_2 from the combination of Raman scattering and *ab initio* structural search

Victor Balédent,[1] Tiago T. F. Cerqueira,[2,3] Rafael Sarmiento-Pérez,[3] Abhay Shukla,[4] Christophe Bellin,[4] Marino Marsi,[1] Jean-Paul Itié,[5] Matteo Gatti,[6,7,5] Miguel A. L. Marques,[8] Silvana Botti,[2] and Jean-Pascal Rueff[5,9]

[1]*Laboratoire de Physique des Solides, CNRS, Université Paris-Sud, Université Paris-Saclay 91405 Orsay Cedex, France*

[2]*Institut für Festkörpertheorie und -optik, Friedrich-Schiller-Universität Jena and European Theoretical Spectroscopy Facility, Max-Wien-Platz 1, 07743 Jena, Germany*

[3]*Institut Lumière Matière, UMR5306 Université Lyon 1-CNRS, Université de Lyon, F-69622 Villeurbanne Cedex, France*

[4]*Institut de Minéralogie, de Physique des Matériaux et de Cosmochimie, UPMC Sorbonne Universités, UMR CNRS 7590, Muséum National d'Histoire Naturelle, IRD UMR 206, Paris 75005, France*

[5]*Synchrotron SOLEIL, Saint-Aubin, Boîte Postale 48, 91192 Gif-sur-Yvette Cedex, France*

[6]*Laboratoire des Solides Irradiés, École Polytechnique, CNRS, CEA, Université Paris-Saclay, F-91128 Palaiseau, France*

[7]*European Theoretical Spectroscopy Facility (ETSF)*

[8]*Institut für Physik, Martin-Luther-Universität Halle-Wittenberg, D-06099 Halle, Germany*

[9]*Laboratoire de Chimie Physique–Matière et Rayonnement, UPMC Sorbonne Universités, UMR CNRS 7614, Paris 75005, France*

(Received 21 March 2016; revised manuscript received 22 December 2017; published 17 January 2018)

Despite more than 50 years of investigation, the understanding of the metal-insulator transition in VO_2 remains incomplete and requires additional experimental and theoretical works. Using Raman scattering under pressure, we first confirm the known transition around 11 GPa affecting the V orbital occupancy in the absence of structural changes. Moreover, we disclose a transition around 19 GPa involving the V orbitals together with a structural distortion, revealed by the splitting of a phonon branch associated with the V chains. The high-pressure metallic *X* phase is found to be of low symmetry and becomes the lowest-enthalpy structure at high pressure by *ab initio* structural prediction calculations. In contrast to a well-established picture of the metal-insulator transition (i.e., the Peierls transition), the high-pressure metallic phase here is of lower symmetry than the ambient pressure insulating phase.

DOI: 10.1103/PhysRevB.97.024107

I. INTRODUCTION

In strongly correlated materials, the intricate interplay among different degrees of freedom (charge, spin, orbital, lattice) gives rise to a large diversity of ground states. Their complex phase diagrams are characterized by a great sensitivity to external parameters leading to large variations of their properties, such as for metal-insulator transitions (MITs) and colossal magnetoresistance, and to the emergence of exotic phenomena such as unconventional superconductivity. These distinctive features naturally make correlated materials very attractive for many promising technological applications. For the same reasons, however, understanding and controlling the transition between different phases still represents a major challenge for condensed-matter physics.

Among the correlated transition-metal oxides, VO_2 is a prototype compound displaying a strong interaction between electronic and structural degrees of freedom. By cooling down below 340 K, a MIT with a change in the resistivity of five orders of magnitude is accompanied by a structural distortion with a doubling of the crystal unit cell from a rutile *R* to a monoclinic M_1 phase [1]. While a strain-controlled MIT was recently demonstrated [2], several works have shown that this twofold transition can also be photoinduced on an ultrafast time scale through a nonequilibrium state [3–10]. The complexity of the phase diagram of VO_2 [11,12] is increased further by Cr doping, which produces two additional insulating phases, namely the monoclinic M_2 and triclinic *T* phases [13,14], and by applying hydrostatic pressure. Indeed, Arcangeletti *et al.* observed a noticeable metallization above 11 GPa [15]. This conductivity increase, revealed by infrared absorption spectroscopy, comes with an enhanced susceptibility of the V chain phonons at high pressure. This has been confirmed by recent x-ray diffraction, reporting a transition at the very same pressure affecting the bulk modulus [16]. It is worth noting that, despite the anisotropic crystal compression, this transition is not accompanied by lattice symmetry breaking. At higher pressure, a recent study shows a further phase transition [17]. The three orders of magnitude drop of the resistivity together with the damped phonon mode in the Raman scattering mode strongly suggest that this *X* phase is metallic.

In the long-standing debate about the theoretical understanding of VO_2, the emphasis has been placed alternatively on the key role played by electronic correlation or by structural distortion [18–22]. Advanced many-body approaches [23–25], beyond density-functional theory (DFT) in the local-density approximation (LDA), were recently able to obtain a description of correlation effects in the electronic excitation spectra in good agreement with photoemission experiments [26]. However, a consistent interpretation within a single theoretical framework of the structural, electronic, and magnetic

properties of VO_2 across the whole phase diagram still remains elusive [27–33].

In the present work, we uncover a different phase transition in VO_2 under high pressure. This M_3 phase emerges at around 19 GPa from the compressed M_1' phase that was previously observed around 11 GPa [15–17,34,35], disclosing a different region of the phase diagram. An unbiased *ab initio* search of the low enthalpy structures using the minima hopping method [36,37] predicts a stable structure at high pressure compatible with the metallic X phase reported in Ref. [17], establishing the minima hopping method as a very promising, predictive tool of investigation for strongly correlated materials.

II. METHODS

A. Experiments

In this work, we used Raman scattering to probe the lattice degrees of freedom as a function of applied pressure at ambient temperature. Experiments were performed with a 534 nm laser source, with a fixed power of 10 mW in a backscattering geometry. VO_2 powder was loaded in a diamond anvil cell using diamonds of 300 μm culet size and an inox gasket drilled with a 150 μm hole. Different transmitting media (silicone oil, neon, and argon) were tested yielding identical results. Since helium is reportedly best for hydrostaticity, we only present spectra obtained with this transmitting medium. We applied pressure ranging from 1 GPa (limited by the gas-loading procedure) to 26 $\pm$ 0.5 GPa. The raw data measured at the two extreme pressure points are presented in Fig. 2. A third-order polynomial background has been removed from the raw data to ease the comparison of the spectra at different pressures in Fig. 1. The background comes from the tail of the elastic line, as can be seen in Fig. 2. It is not particularly intense despite the backscattering geometry. The width of the Raman peak at low pressure in VO_2 is comparable to that measured in a Si single crystal used as a reference. This shows that the peak shape is limited by resolution and justifies using a Gaussian line shape for the fits.

To confirm the structural change, we performed x-ray diffraction experiment at PSICHÉ beamline at Synchrotron SOLEIL using neon as a pressure-transmitting medium. The gas-loading system for the diamond anvil cell fixed the pressure starting point at 8.6 GPa. Pressure determination was identical to the Raman experiment method using ruby fluorescence, and it has been corroborated thanks to the known neon equation of state [38] combined with observed neon diffraction peaks. Both methods give the same pressure estimation within error bars of less than 0.5 GPa.

B. Theory

To identify the crystal structure of the high-pressure phases, we performed structural search simulations for cells containing up to six formula units of VO_2. Given only the chemical composition of a system, the structural search algorithm aims at finding the global minimum on the enthalpy surface while gradually exploring low-lying structures. We used the minima hopping method (MHM), which has already been used with remarkable success in a wide range of applications [39–41], including the dependence on pressure [42] and the exploration

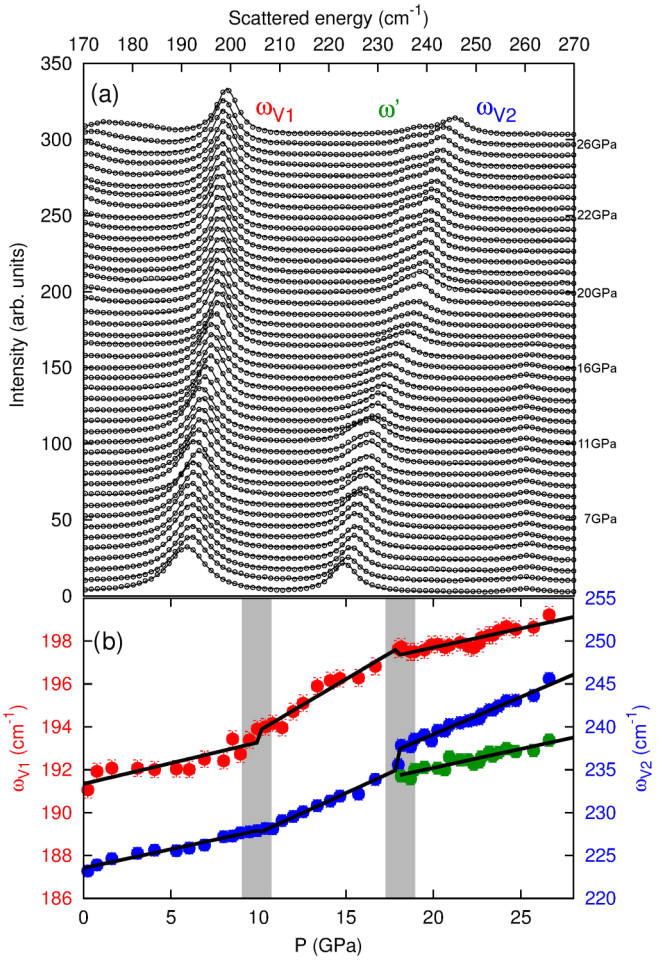

FIG. 1. (a) Raman spectra for pressure from 1 GPa (bottom) to 26 GPa (top) (open circles) and associated Gaussian fit (lines) at room temperature. The spectra show the two phonons associated with the V chains (ω_{V1} = 191 cm^{-1} and ω_{V2} = 222 cm^{-1} at ambient pressure). (b) Evolution of the ω_{V1} (red points, left scale) and the ω_{V2} (blue points, right scale) modes as a function of pressure. The split mode ω_V' observed above ~19 GPa is shown in green (right scale).

of binary phase diagrams [43]. However, to the best of our knowledge, no *ab initio* crystal structure prediction algorithm has been applied so far to study phase transitions in strongly correlated materials.

We note that at ambient pressure the calculated cell volumes of ferromagnetic or antiferromagnetic phases are closer to the measured cell volume for the paramagnetic metal than the volume obtained from a spin-unpolarized calculation, as was also discussed in Ref. [31]. In that work, it was concluded that spin-polarized calculations should always be performed if the focus is on structural properties, despite the fact that the magnetic ordering is not observed in experiments. This fact suggests indeed that either there are disordered local spin moments in rutile VO_2 or that the inclusion of spin polarization compensates for the poor description of strong correlation. In our structural prediction runs with the minima hopping method, we observed that low-enthalpy structures with different symmetries were obtained by imposing spin-polarized or spin-unpolarized solutions. As we are interested

in obtaining reliable crystal structures, and in agreement with Ref. [31], in the following we will present spin-polarized calculations.

The initial geometries for the MHM runs were obtained randomly, ensuring only that the minimal distance between the atoms was at least equal to the sum of the covalent radii. Moves on the enthalpy surface are performed by combining consecutive short molecular dynamics escape steps with local geometry relaxations, taking into account both atomic and cell variables. The initial velocities for the molecular-dynamics trajectories are chosen approximately along soft-mode directions, thus allowing efficient escapes from local minima and aiming toward low-energy structures. We performed a complete structural search study at 0 and 25 GPa. In a second stage, the lowest-enthalpy structures identified at 0 and 25 GPa were reoptimized from 0 to 26 GPa with steps of 2 GPa in order to follow the evolution of each structure with pressure.

During the runs, forces and energies were obtained in the DFT framework using the projector-augmented-wave method [44] as implemented in VASP [45,46]. We used the Perdew-Burke-Ernzerhof (PBE) approximation [47] to the exchange-correlation functional together with an on-site Coulomb repulsive interaction U [48] of 3 eV to correct the V d states. While it is well known that these functionals are not entirely reliable for the description of the band structures or the magnetic properties of VO_2 [20,21,29,32,33], here the focus is on finding the ground-state crystal structure as a function of pressure [31]. The plane-wave cutoff was set to 400 eV and the number of k points in the direction $\mathbf{b}_i$ was given by $|b_i|/(0.03 \times 2\pi)$, where $\mathbf{b}_i$ is the reciprocal-lattice vector. The resulting structures were then reoptimized by ensuring numerical convergence to less than 2 meV at^{-1} by using automatically determined dense k-point grids and a plane-wave cutoff of 520 eV.

III. RESULTS AND DISCUSSION

A. Raman spectroscopy

We acquired the spectra from 100 to 1000 cm^{-1} to access the totality of the Raman-active phonons branches with a specific focus on the low-energy region between 170 and 270 cm^{-1}. The spectra are presented in Fig. 1(a) (black circles) after background subtraction for pressures ranging from 1 (bottom spectra) to 26 GPa (top spectra) in steps of ∼0.5 GPa. To extract the Raman peak positions, the spectra were fitted to the sum of Gaussian line shapes (black lines); fitting with Voigt line shapes yields indiscernible results. Two peaks are visible at low pressure in this selected range of energy, labeled, respectively, ω_{V1} and ω_{V2}. These are associated with the vanadium chains [15]. The fitted value of the frequency is shown in Fig. 1(b) for both phonon branches. We notice a sudden change of slope at 10 GPa for both modes. This confirms the results reported in [15]. More interestingly, a second anomaly that has remained unnoticed so far is found around 19 GPa. While the slope of the ω_{V1} mode retrieves its low-pressure value, the second mode ω_{V2} splits, giving rise to an additional mode labeled ω'_V in Fig. 1(a). It is the combination of both effects (peak splitting and slope change) that establishes the transition pressure at 19 GPa. The 19 GPa anomaly is a signature of the interplay between electronic and structural degrees of freedom. This raises the question of the nature of this anomaly, defining or not a true phase transition with an order parameter and a symmetry breaking.

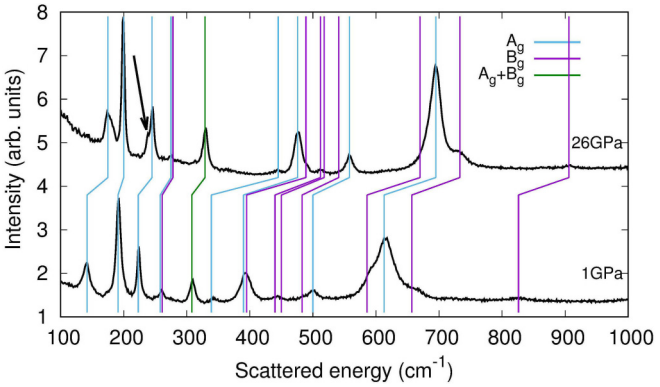

FIG. 2. Assignment of the phonon symmetry for 1 GPa (bottom) and 26 GPa (top) Raman spectra at room temperature. As predicted by group theory, nine A_g and nine B_g symmetry branches are identified by the blue and red discontinuous lines, respectively. The split branch at 236 cm^{-1} pointed out by the black arrow does not come from a preexisting phonon at ambient pressure. This increase in the number of vibrational modes indicates the symmetry breaking of the lattice.

To get further insight into this phase transition, we now turn to the total phonon spectra. The extended spectra are shown in Fig. 2 for 1 and 26 GPa. According to group theory applied to the lattice symmetry of VO_2, we expect nine optical modes with A_g symmetry and nine for B_g symmetry. A comparison of our low-pressure spectra with those reported in Refs. [49,50] enables a complete assignment of these 18 phonons. In Fig. 2, the A_g and B_g modes are shown by dashed blue and red lines, respectively, and the mixed A_g and B_g modes are shown by a green dashed line. All the low-pressure phonons persist up to 26 GPa except for the onset of the branch ω'_V pointed out by the black arrow, which cannot be ascribed to a preexisting mode. This proves unambiguously that there is an new vibrational mode in the Raman spectra above 19 GPa.

B. X-ray diffraction

The modification of the number of phonons is a fingerprint of a structural transition breaking the lattice symmetry or of the coexistence of phases as recently suggested by structural calculation [51]. As displayed in Fig. 3, the diffractogram shows no indications of a space-group change through 11 GPa, confirming the previous results [16,17]. However, a clear distortion of the diffractogram from 14.7 to 20.8 GPa is visible with the splitting of the Bragg peaks at 8° and 13° associated with the vanadium position. We also note that our diffraction data up to 37 GPa show no sign of the X metallic phase, at odds with the results of Ref. [17]. We assign this discrepancy to a possible underestimation of pressure in Ref. [17]. A revised estimate of the pressure from the neon diffraction peaks of Ref. [17] indicates a structural transition at 40 GPa when using the known neon equation of state [38]. This value is about 10 GPa higher than reported. In our case, both ruby fluorescence and neon diffraction are consistent.

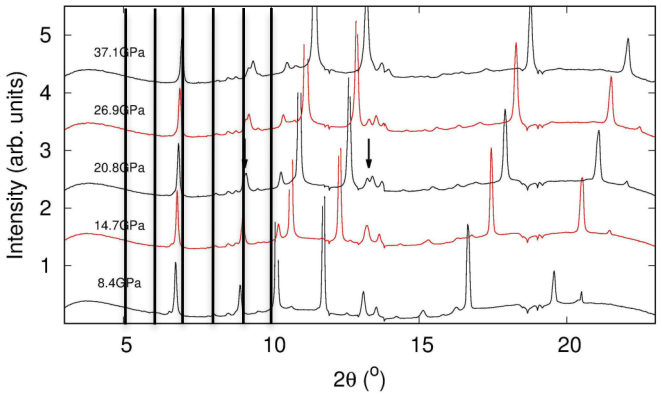

FIG. 3. High-pressure diffractogram of VO_2. The arrows show the splitting of the Bragg peaks around 20 GPa.

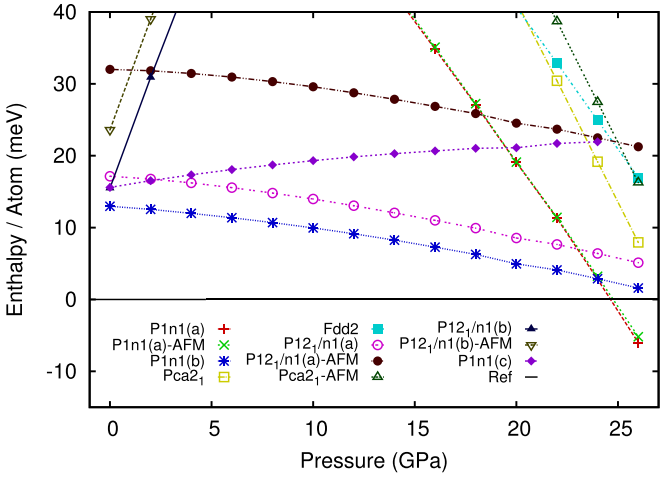

FIG. 4. Enthalpy per atom of the low-energy VO_2 crystal structures as a function of pressure with respect to the ground-state (at zero pressure) reference phase (M_1, space group $P2_1/c$).

Therefore, the x-ray diffraction results confirm the conclusions based on Raman spectra of Sec. III A that a structural modification occurs around 19 GPa involving vanadium atoms. The XRD anomaly in Fig. 3 indicates that either symmetries are broken or an another phase settles above 19 GPa or coexists with the previous one. In any case, the space group of the M_3 phase has to be compatible with the mean space group of the low-pressure phase. It is likely that a minute change of the vanadium dimers symmetry is at work. This interpretation is further supported by the theoretical work in Ref. [51]. As the Raman spectra remain undamped, we can definitely conclude that the M_3 phase stays insulating and cannot be the metallic X phase but rather is an intermediate phase.

Unfortunately, it was not possible to determine precisely the atomic crystal positions through a Rietveld refinement of the XRD experimental data due to the broadening of the peaks under pressure and weak oxygen contribution and the intrinsic difficulty of the diffraction experiment on VO_2, which is composed by two light elements. Similar problems are common for this kind of experiment [16,17]. High-pressure single-crystal diffraction would be required for the exact determination of the crystal structure of the M_3 phase. This is, however, beyond the scope of the present work, which reveals the existence of the M_3 phase. We believe that the present results will thus stimulate new experiments, which should be carefully done in a 15–25 GPa range of pressures, in order to investigate in detail the structural and electronic properties of the M_3 phase.

C. *Ab initio* structural search simulations

At the same time, the experimental difficulties in identifying the precise crystal structures of the high-pressure phases of VO_2 suggest the need to undertake a complementary *ab initio* theoretical simulation to search for the most stable crystal structures as a function of pressure.

In Fig. 4 we show the enthalpy as a function of pressure of the lowest-enthalpy phases found by our unbiased MHM simulations. The zero is set to the enthalpy of the most stable structure at $T = 0$ K and ambient pressure. This structure corresponds to the experimental M_1 ($P12_1/n1$, space group 14), even if in our structural reoptimization it gets symmetrized to the tetragonal structure R ($P4/mnm$,136) [29,32,33,52,53].

We notice that the energy difference between the M_1 and the R crystal structures is within the accuracy of our calculations. Moreover, within a small energy range of 30 meV per atom (i.e., the same order of k_BT at room temperature) we find four other monoclinic structures with space group 14 or 7. Two almost degenerate monoclinic $P1n1$ structures (space group 7), one of which is ferromagnetic and the other is antiferromagnetic, enter the graph at about 15 GPa. They display a much more dispersive enthalpy curve as their volume is about 10% smaller than the volume of the M_1 phase and of the other low-lying monoclinic phases with flatter enthalpy lines. The enthalpy of the $P1n1$ structure crosses the M_1 reference curve at 24–26 GPa, where this less symmetric crystal becomes the lowest enthalpy structure.

We remark that this structural transition is driven by the volume difference between the two structures, due to the pV term in the enthalpy. Therefore, even though the value of pressure of the transition may depend on the precision of the total energy calculation, the existence of the phase transition itself is in any case ensured by the volume differences, independently of the approximation used. This was confirmed by calculations using the standard PBE functional (i.e., setting $U = 0$). In Fig. 5 we present the enthalpy curves obtained with the spin-polarized PBE functional with $U = 0$. At low pressure, the results differ from experimental data, motivating the use of PBE+U to account for the localized nature of V $3d$ electrons. More interestingly, for the topic of the present work, at high pressure ($P > 25$ GPa) the $P1n1$ structure (red curve in Fig. 5) becomes the most stable also with the PBE functional. This demonstrates that, even though the transition pressure may depend on the precision of the total energy calculation, the structural transition itself is independent of the approximation used, as is driven by volume differences in the pV term of the enthalpy.

The simulated diffraction pattern obtained for this $P1n1$ structure is not compatible with the one observed above 19 GPa. However, it matches well with the experimental diffractogram of the metallic X phase [17]. The calculation method could not predict the intermediary phase M_3 as it would require a computational accuracy of the internal energy that is

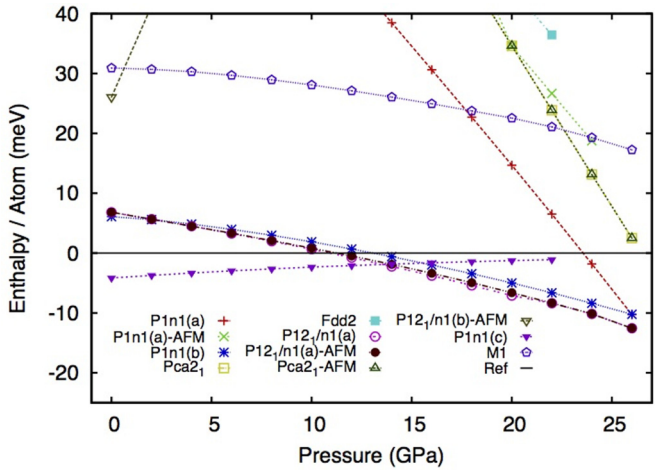

FIG. 5. Enthalpy per atom of the low-energy VO_2 crystal structures as a function of pressure calculated with the PBE functional. The zero corresponds to the rutile structure at ambient pressure.

beyond reach at the moment. This is supported by the recent theoretical work [51] showing a coexistence of two nearly degenerate phases. We can also expect from Fig. 4 that at higher pressures other structures will become more stable than the X structure.

We can now compare the M_1 and the X monoclinic structures; see Fig. 6. Both atomic arrangements are obtained as distortions of the rutile structure. However, in X the distortion is more accentuated and we can find V atoms that are sevenfold-coordinated, instead of sixfold-coordinated. This implies the presence of threefold-coordinated O atoms. We note that in the rutile structure there are two different V-O bond lengths (at 26 GPa): 1.93 Å (four bonds) and 1.85 Å (two bonds). Due to the reduced symmetry, in the X phase all bond lengths are different, with values ranging from 1.90 to 2.13 Å. We checked the dynamical stability of the most stable crystal structures at different pressures by performing phonon calculations. The phonon band structure and phonon density of states of the candidate $P1n1(a)$ structure for the X monoclinic phase are shown in Fig. 7.

Incidentally, we would like to mention the low-pressure $P12_1/n1$ phases. These have a considerably larger volume than the reference phase and become the ground state at a negative pressure of around -2 GPa (see Fig. 4). It is conceivable that this structure is experimentally accessible by either growing

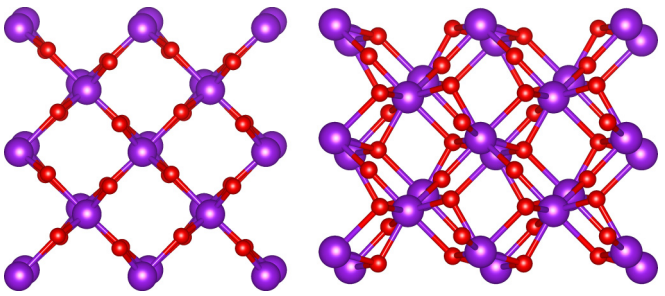

FIG. 6. Structure of monoclinic M_1 VO2 (left) compared with the new monoclinic M_3 phase ($P1n1$) (right).

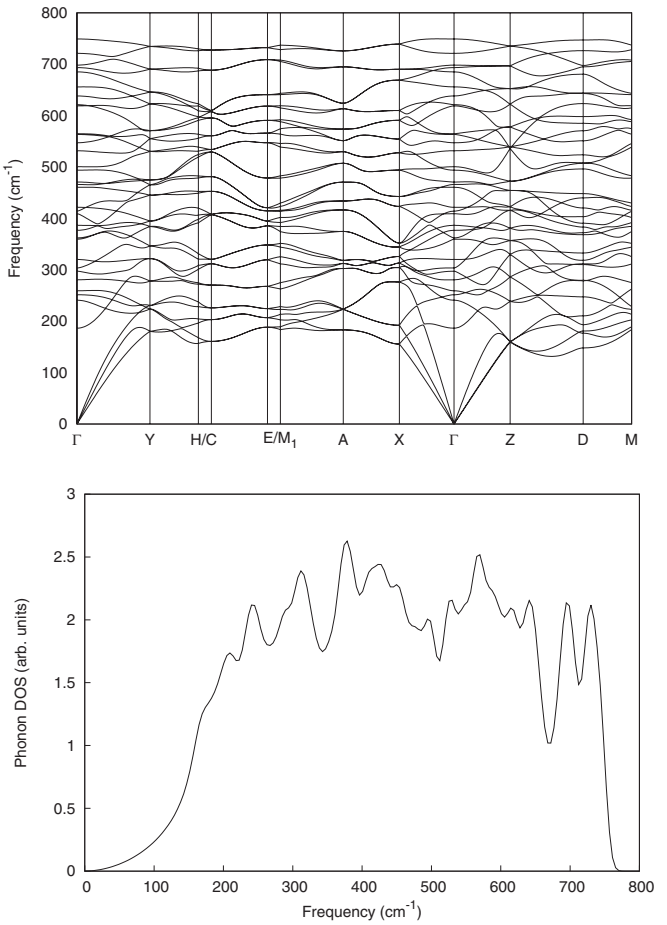

FIG. 7. Phonon band structure and density of states for the X monoclinic phase.

VO_2 in a compatible substrate with a slightly larger lattice constant or by doping with appropriate larger atoms.

IV. CONCLUSIONS

In summary, by Raman scattering and x-ray diffraction experiments under pressure, we identified two phase transitions of VO_2 in which the electronic and structural degrees of freedom appear to be decoupled, in contrast to the MIT at ambient pressure. In addition to the anomaly at 11 GPa that has an electronic nature as previously reported [15,16], we have unambiguously discovered another M_3 phase developing above 19 GPa that breaks the lattice symmetry. The M_3 phase intercalates between the M_1' and the metallic X phases as a different phase, recalling the intermediate T phase between M_1 and M_2 in Cr-doped VO_2 [13,14]. By performing an *ab initio* structural search, we found that the high-pressure metallic X phase is likely to be a monoclinic structure with a lower symmetry than the M_1 phase. Furthermore, our results reveal that the intermediate phase M_3 can alter the vanadium dimers while remaining insulating. Second, the monoclinicity of the high-pressure X metallic phase contrasts with the rutile structure of the ambient pressure metallic phase. These high-pressure phases thus appear as a critical test of competing theoretical models of the MIT at ambient pressure.

Overall, our findings put forward the combination of x-ray diffraction, Raman scattering, and minima hopping as a very promising tool of investigation for the complex phase diagrams of strongly correlated oxides. They also call for complementary experiments to refine the electronic and structural properties of VO_2 at high pressure.

ACKNOWLEDGMENTS

This research was supported by a Marie Curie FP7 Integration Grant within the Seventh European Union Framework Programme, and partially supported by the Région Ile-de-France through the program DIM OxyMORE.

[1] F. Morin, Phys. Rev. Lett. **3**, 34 (1959).
[2] N. B. Aetukuri, A. X. Gray, M. Drouard, M. Cossale, L. Gao, A. H. Reid, R. Kukreja, H. Ohldag, C. A. Jenkins, E. Arenholz, K. P. Roche, H. A. Durr, M. G. Samant, and S. S. P. Parkin, Nat. Phys. **9**, 661 (2013).
[3] A. Cavalleri, C. Tóth, C. W. Siders, J. A. Squier, F. Ráksi, P. Forget, and J. C. Kieffer, Phys. Rev. Lett. **87**, 237401 (2001).
[4] A. Cavalleri, T. Dekorsy, H. H. W. Chong, J. C. Kieffer, and R. W. Schoenlein, Phys. Rev. B **70**, 161102 (2004).
[5] P. Baum, D.-S. Yang, and A. H. Zewail, Science **318**, 788 (2007).
[6] C. Kübler, H. Ehrke, R. Huber, R. Lopez, A. Halabica, R. F. Haglund, Jr., and A. Leitenstorfer, Phys. Rev. Lett. **99**, 116401 (2007).
[7] S. Wall, D. Wegkamp, L. Foglia, K. Appavoo, J. Nag, R. Haglund, J. Stähler, and M. Wolf, Nat. Commun. **3**, 721 (2012).
[8] D. Wegkamp, M. Herzog, L. Xian, M. Gatti, P. Cudazzo, C. L. McGahan, R. E. Marvel, R. F. Haglund, A. Rubio, M. Wolf, and J. Stähler, Phys. Rev. Lett. **113**, 216401 (2014).
[9] V. R. Morrison, R. P. Chatelain, K. L. Tiwari, A. Hendaoui, A. Bruhács, M. Chaker, and B. J. Siwick, Science **346**, 445 (2014).
[10] D. Wegkamp and J. Stähler, Prog. Surf. Sci. **90**, 464 (2015).
[11] J. H. Park, J. M. Coy, T. S. Kasirga, C. Huang, Z. Fei, S. Hunter, and D. H. Cobden, Nature (London) **500**, 431 (2013).
[12] J. Laverock, S. Kittiwatanakul, A. A. Zakharov, Y. R. Niu, B. Chen, S. A. Wolf, J. W. Lu, and K. E. Smith, Phys. Rev. Lett. **113**, 216402 (2014).
[13] M. Marezio, D. B. McWhan, J. P. Remeika, and P. D. Dernier, Phys. Rev. B **5**, 2541 (1972).
[14] D. B. McWhan, M. Marezio, J. P. Remeika, and P. D. Dernier, Phys. Rev. B **10**, 490 (1974).
[15] E. Arcangeletti, L. Baldassarre, D. Di Castro, S. Lupi, L. Malavasi, C. Marini, A. Perucchi, and P. Postorino, Phys. Rev. Lett. **98**, 196406 (2007).
[16] M. Mitrano, B. Maroni, C. Marini, M. Hanfland, B. Joseph, P. Postorino, and L. Malavasi, Phys. Rev. B **85**, 184108 (2012).
[17] L. Bai, Q. Li, S. A. Corr, Y. Meng, C. Park, S. V. Sinogeikin, C. Ko, J. Wu, and G. Shen, Phys. Rev. B **91**, 104110 (2015).
[18] J. B. Goodenough, J. Solid State Chem. **3**, 490 (1971).
[19] A. Zylbersztejn and N. F. Mott, Phys. Rev. B **11**, 4383 (1975).
[20] R. M. Wentzcovitch, W. W. Schulz, and P. B. Allen, Phys. Rev. Lett. **72**, 3389 (1994).
[21] V. Eyert, Ann. Phys. **11**, 650 (2002).
[22] J. D. Budai, J. Hong, M. E. Manley, E. D. Specht, C. W. Li, J. Z. Tischler, D. L. Abernathy, A. H. Said, B. M. Leu, L. A. Boatner, R. J. McQueeney, and O. Delaire, Nature (London) **515**, 535 (2014).
[23] S. Biermann, A. Poteryaev, A. I. Lichtenstein, and A. Georges, Phys. Rev. Lett. **94**, 026404 (2005).
[24] M. Gatti, F. Bruneval, V. Olevano, and L. Reining, Phys. Rev. Lett. **99**, 266402 (2007); M. Gatti, G. Panaccione, and L. Reining, *ibid.* **114**, 116402 (2015).
[25] C. Weber, D. D. O'Regan, N. D. M. Hine, M. C. Payne, G. Kotliar, and P. B. Littlewood, Phys. Rev. Lett. **108**, 256402 (2012).
[26] T. C. Koethe, Z. Hu, M. W. Haverkort, C. Schüßler-Langeheine, F. Venturini, N. B. Brookes, O. Tjernberg, W. Reichelt, H. H. Hsieh, H.-J. Lin, C. T. Chen, and L. H. Tjeng, Phys. Rev. Lett. **97**, 116402 (2006).
[27] V. Eyert, Phys. Rev. Lett. **107**, 016401 (2011).
[28] R. Grau-Crespo, H. Wang, and U. Schwingenschlögl, Phys. Rev. B **86**, 081101 (2012).
[29] X. Yuan, Y. Zhang, T. A. Abtew, P. Zhang, and W. Zhang, Phys. Rev. B **86**, 235103 (2012).
[30] Z. Zhu and U. Schwingenschlögl, Phys. Rev. B **86**, 075149 (2012).
[31] B. Xiao, J. Sun, A. Ruzsinszky, and J. P. Perdew, Phys. Rev. B **90**, 085134 (2014).
[32] H. Zheng and L. K. Wagner, Phys. Rev. Lett. **114**, 176401 (2015).
[33] H. Wang, T. A. Mellan, R. Grau-Crespo, and U. Schwingenschlögl, Chem. Phys. Lett. **608**, 126 (2014).
[34] C. Marini, E. Arcangeletti, D. Di Castro, L. Baldassare, A. Perucchi, S. Lupi, L. Malavasi, L. Boeri, E. Pomjakushina, K. Conder, and P. Postorino, Phys. Rev. B **77**, 235111 (2008).
[35] C. Marini, M. Bendele, B. Joseph, I. Kantor, M. Mitrano, O. Mathon, M. Baldini, L. Malavasi, S. Pascarelli, and P. Postorino, Europhys. Lett. **108**, 36003 (2014).
[36] S. Goedecker, J. Chem. Phys. **120**, 9911 (2004).
[37] M. Amsler and S. Goedecker, J. Chem. Phys. **133**, 224104 (2010).
[38] R. J. Hemley, C. S. Zha, A. P. Jephcoat, H. K. Mao, L. W. Finger, and D. E. Cox, Phys. Rev. B **39**, 11820 (1989).
[39] M. Amsler, J. A. Flores-Livas, L. Lehtovaara, F. Balima, S. A. Ghasemi, D. Machon, S. Pailhès, A. Willand, D. Caliste, S. Botti, A. San Miguel, S. Goedecker, and M. A. L. Marques, Phys. Rev. Lett. **108**, 065501 (2012).
[40] T. D. Huan, M. Amsler, M. A. L. Marques, S. Botti, A. Willand, and S. Goedecker, Phys. Rev. Lett. **110**, 135502 (2013).
[41] M. Amsler, S. Botti, M. A. L. Marques, and S. Goedecker, Phys. Rev. Lett. **111**, 136101 (2013).
[42] J. A. Flores-Livas, M. Amsler, T. J. Lenosky, L. Lehtovaara, S. Botti, M. A. L. Marques, and S. Goedecker, Phys. Rev. Lett. **108**, 117004 (2012).
[43] R. Sarmiento-Pérez, T. F. T. Cerqueira, I. Valencia-Jaime, M. Amsler, S. Goedecker, S. Botti, M. A. L. Marques, and A. H. Romero, New J. Phys. **15**, 115007 (2013).
[44] P. E. Blöchl, Phys. Rev. B **50**, 17953 (1994).
[45] G. Kresse and J. Furthmüller, Comput. Mater. Sci. **6**, 15 (1996).
[46] G. Kresse and J. Furthmüller, Phys. Rev. B **54**, 11169 (1996).

[47] J. P. Perdew, K. Burke, and M. Ernzerhof, Phys. Rev. Lett. **77**, 3865 (1996).
[48] V. I. Anisimov, J. Zaanen, and O. K. Andersen, Phys. Rev. B **44**, 943 (1991).
[49] X.-B. Chen, J. Korean Phys. Soc. **58**, 100 (2011).
[50] K. Hyun-Tak, C. Byung-Gyu, Y. Doo-Hyeb, K. Gyungock, K. Kwang-Yong, L. Seung-Joon, K. Kwan, and L. Yong-Sik, Appl. Phys. Lett. **86**, 242101 (2005).
[51] H. He, H. Gao, W. Wu, S. Cao, J. Hong, D. Yu, G. Deng, Y. Gao, P. Zhang, H. Luo, and W. Ren, Phys. Rev. B **94**, 205127 (2016).
[52] A. Jain, S. P. Ong, G. Hautier, W. Chen, W. D. Richards, S. Dacek, S. Cholia, D. Gunter, D. Skinner, G. Ceder, and K. A. Persson, APL Mater. **1**, 011002 (2013).
[53] J. Saal, S. Kirklin, M. Aykol, B. Meredig, and C. Wolverton, JOM **65**, 1501 (2013).